

Article

Segregation Modeling in Stockpile Using Discrete Element Method

René Gómez ^{1,*} , Krzysztof Skrzypkowski ^{2,*} , Manuel Moncada ¹ , Raúl Castro ³ and Rodrigo Lazo ⁴ ¹ Faculty of Engineering, Universidad de Concepcion, Concepción 4030000, Chile² Faculty of Civil Engineering and Resource Management, AGH University of Science and Technology, 30-059 Kraków, Poland³ Advanced Mining Technology Center, Universidad de Chile, Santiago 8370451, Chile⁴ Sustainable Mine Planning, Santiago 4070371, Chile

* Correspondence: regomez@udec.cl (R.G.); skrzypko@agh.edu.pl (K.S.)

Abstract: During stockpile feeding, the small particles migrate to the center of the stock while large particles end up around the edges. This phenomenon influences how the mineral is fragmented in the subsequent stages of size reduction. In this study, the primary variables involved in this phenomenon were studied using the discrete element to simulate particle segregation. Results show that the ratio between coarse and fine particles strongly affects particle segregation. The segregation phenomenon was not observed when there were fewer coarse particles in the mix. The feeding height was also found to influence segregation and to affect the angles of repose and dumping. Finally, the rounded polyhedral shape of particles generated the simulation performance most similar to actual particle segregation based on a case study analyzed.

Keywords: discrete element method; granular material; gravity flow; mining; stockpile



Citation: Gómez, R.; Skrzypkowski, K.; Moncada, M.; Castro, R.; Lazo, R. Segregation Modeling in Stockpile Using Discrete Element Method. *Appl. Sci.* **2022**, *12*, 12449. <https://doi.org/10.3390/app122312449>

Academic Editors: Susana Lopez-Querol and Pedro Navas

Received: 14 November 2022

Accepted: 29 November 2022

Published: 5 December 2022

Publisher's Note: MDPI stays neutral with regard to jurisdictional claims in published maps and institutional affiliations.



Copyright: © 2022 by the authors. Licensee MDPI, Basel, Switzerland. This article is an open access article distributed under the terms and conditions of the Creative Commons Attribution (CC BY) license (<https://creativecommons.org/licenses/by/4.0/>).

1. Introduction

In mining, a stockpile is a storage location of ore, which is reserved to be later sent to stages of size reduction and subsequent mineral processing in the plant. During the stockpiling process, segregation and stratification occur spontaneously, leading directly to a state of particulate system division [1]. In stockpiles, size segregation can limit temporal control of the material placed in the pile without knowing its tonnage and grade requirements. In addition, this segregation implies that when unloading from the bottom of the stockpile, there will be a greater flow of fine particles initially that will then subsequently change to a more significant coarse particle flow. Variations in the particle size of the extracted ore due to segregation in stockpiles can result in significant fluctuations in the performance of the comminution circuit [2].

Various methods have been used to study the segregation of granular material; these include experimental and numerical methods such as the discrete element method and cellular automata. For example, Cabrejos [3] presented a physical model that can determine how fine materials with high moisture content affect the flowability of most ores in piles, favoring the appearance of arches and ratholes. Ye et al. [4] developed a laboratory test to quantify an ore pile's propensity to segregate. Their results indicated it is possible to quantify size segregation in the laboratory and scale up the results under the experimental conditions used.

In recent years, numerical methods such as cellular automata have been used to simulate the segregation in stockpiles in shorter simulation times. Tien-Fu [5] developed a model based on cellular automata performing various stockpile simulations to know the distribution of grades present in each sector of the pile. The main output parameter of the program is information to identify in which sectors of the stockpile the highest grades are concentrated. Castro et al. [6] proposed a small-scale, quasi-two-dimensional physical

model and a mathematical model based on cellular automata; both were used to investigate size segregation during stacking and gravitational reclaim of stockpiles. Stratification patterns were observed during stockpile formation both in the physical model and in the cellular automaton-based model. Furthermore, the cellular automaton-based model successfully simulated segregation phenomena during gravitational discharging and the topological features of segregation during stockpiling and reclaim. Ye et al. [7] proposed a 3D cellular automaton (CA) model of ore pile formation incorporating size segregation due to surface stratification. The model was found to adequately describe the segregation behavior at a range of model scales, where coarse particles were rolled to the outside of the pile and fine particles were concentrated at the center of the pile. Moreover, the model is fast enough to be used in real-time applications such as dynamic process control and digital twins.

On the other hand, the discrete element method (DEM) has been employed due to its ability to model the physical behavior of particles with great precision and to control a large number of variables, including complex particles' shape [8] and interparticle friction [9]. Yu et al. [10] developed an experimental model with a simulation using the DEM. Using symmetric models, they validated the discrete element method as a viable option for studying the process of stockpile formation. Zhan et al. [1] proposed a 3D-DEM model to study stockpile segregation. This model used two characteristic particle sizes of spheres to separate between fine and coarse particles, where the main variations were in the percentage of the mixture of fine and coarse particles with an experiment of discharge height. This research determined that particles with a higher percentage of coarseness had a higher segregation index. Vuilloz et al. [11] proposed a 2D and 3D stockpile DEM simulation with spherical particles in the contact dynamics approach framework to simulate particle segregation by varying the mixing ratio between fine and coarse particles. The preliminary results of this study established that a greater separation between particles is observed when there is a higher percentage of coarse particles.

Few studies have analyzed the influences of relevant variables (e.g., particle shape, feeding height, and particle sizes) in stockpile during feeding and discharge; these variables can be correctly simulated using the DEM. The DEM has been used successfully to replicate segregation in stockpiles [1,12]. In this work, stockpile segregation was studied through the discrete element method using the software Rocky DEM. Here, a sensibility analysis was performed by changing not only discharge heights, material mixture, and sizes, but also particle shapes to study the influence of all these variables on the segregation process during feeding and discharge.

2. Numerical Model

In the DEM, the contact forces are calculated from a contact model. The normal contact forces (S_n) are defined through the normal superposition of the particles, whereas the tangential forces (S_t) are determined through the tangential superposition [13,14]. In this study, the models used were the hysteretic linear spring model to calculate the normal repulsion force, the linear spring Coulomb limit model to calculate the tangential force, and a constant model to calculate the adhesion force. Simulations were conducted using Rocky DEM software version 4.2.0, widely used in granular material simulations [15–19].

Figure 1 shows an example of the stockpile model simulated through the DEM in this study. The model is composed of the following:

- A feeding zone: Here, particles fall to form a pile. This zone is located at a height H (input variable) over the model floor.
- A base: This zone has two components: a square box ($3\text{ m} \times 3\text{ m}$), where the falling particles form the stockpile, and a feeder ($0.12\text{ m} \times 0.15\text{ m}$) located on the floor of the base's box below the stockpile. The feeder is opened once the stockpile is formed and there are no falling particles from the feeding zone. The discharge from the feeder forms an internal repose angle in the center of the stockpile here called "flow angle".

- Control zone: This zone is located below the base, directly under the feeder zone. The control zone is used to analyze output variables such as the mass drawn and particle size.

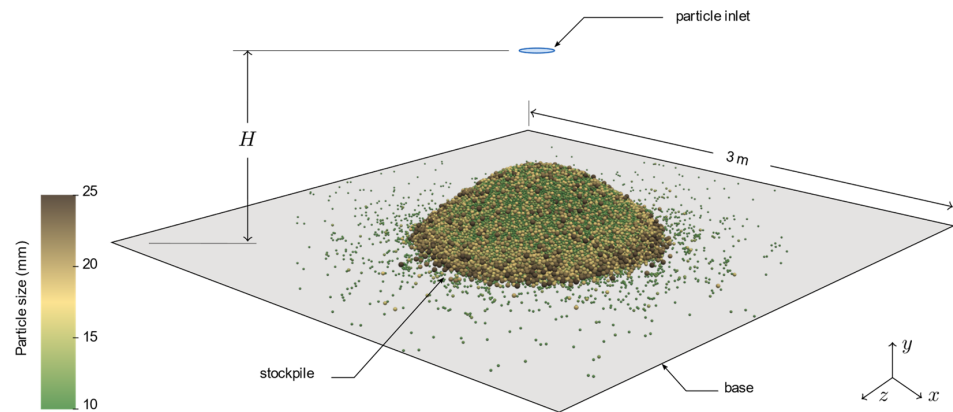


Figure 1. Stockpile model example used in the simulation.

2.1. Input Variables and Numerical Parameters

The following input variables were used in the study:

- Coefficient of Uniformity (CU): Two different PSDs were tested and characterized through their CU (1:2.5).
- Feeding height (H): Different heights were tested to observe their influence on segregation [1]. Heights tested were 1 m, 2 m, and 3 m.
- Coarse to fine particle ratio: Two coarse/fine particle ratios were tested: 70/30% and 60/40%.
- Particle shape: Sphere-shaped particles were initially used and calibrated. Other particle shapes were subsequently simulated to analyze their influence on segregation.
- Number of particles: The number of particles was varied based on the PSD and the coarse-to-fine particle ratio used.

Table 1 summarizes the input variables and the experimental plan (tests) simulated through the DEM. The fine particle sizes are defined based on the study; here, particles below 11.8 mm were defined as fine particles. The PSDs used in the tests are shown in Figure 2.

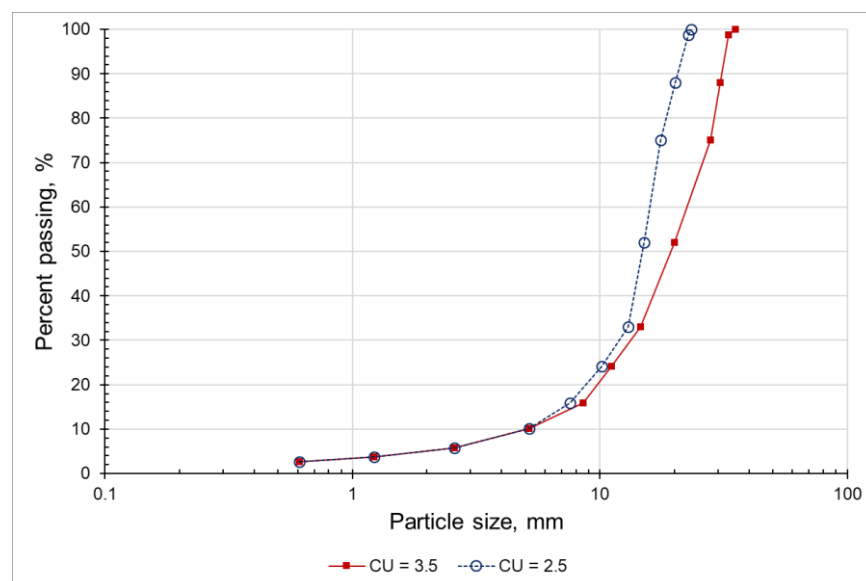


Figure 2. Particle size distributions used in tests.

Table 1. Input variables used in the experimental plan.

Test	Loading Height	CU	Coarse/Fine Particles	Particle Shape		Number of Particles				
				ID	Geometry	Coarse	Fine			
1	1	2.5	70/30	S		81,078	34,748			
2	2	2.5				81,078	34,748			
3	3	2.5				81,078	34,748			
4	1	3.5				79,443	34,047			
5	2	3.5				79,443	34,047			
6	2	3.5				79,443	34,047			
7	1	2.5				81,139	54,093			
8	2	2.5				81,139	54,093			
9	3	2.5				81,139	54,093			
10	1	3.5				60/40	RC		80,206	53,471
11	2	3.5							80,206	53,471
12	3	3.5							80,206	53,471
13	1	2.5	81,078	34,748						
14	1	2.5	70/30	RPg		81,078	34,748			
15	1	2.5				RPd		81,078	34,748	
16	1	2.5						B		81,078

Additionally, the software used the following parameters that had to be defined and calibrated:

- Force fraction: parameter that multiplies the gravity force (9.8 m/s^2) to calculate the force of adhesion (S_n) between particles.
- Adhesion distance: parameter that defines the distance of overlap between particles; used to determine the force of adhesion.
- Dynamic friction (μ_D): parameter to calculate the friction between particles during movement.
- Static friction (μ_S): parameter to calculate the friction between particles in static conditions.
- Rolling friction (μ_R): parameter used to include a contact moment in the opposite direction of rotation.

Some software parameters were defined based on similar studies [10,11]:

- Elastic moduli: the stiffness of particles and surfaces.
- Density: the mass of a particle volume.
- Restitution coefficient: energy dissipated between contacts.

2.2. Output Variables

The following variables were used to analyze the segregation phenomenon in a stockpile:

- Repose angle: natural angle formed by the stockpile during particle feeding.
- Flow angle: internal angle formed in the center of the pile during particle discharge.
- Total and live capacities: mass of particles in the stockpile before and after discharge.
- PSD during discharge: particle size distribution (PSD) measured in the control zone.

Additionally, different stockpile views were used to observe the visual segregation observed in previous studies [20,21].

3. Calibration

A based case from a stockpile was used to calibrate the numerical model. Table 2 shows the variables used to calibrate the model. In this calibration stage, the numerical parameters were calibrated for sphere particle shape. The following particle shapes tested were simulated with the same calibrated parameters. Figure 1 shows the model used during the calibration stage.

Table 2. Rock characteristics obtained from a stockpile.

Parameters	Value	Unit
Rock size min/max	10.1/25.4	mm
Repose angle	32	°
Bulk density	1.62	t/m ³

The numerical parameters were calibrated minimizing the square error of the repose angle using Equation (1),

$$Error = \frac{\sqrt{\sum_{i=1}^n (M - O)^2}}{n} \quad (1)$$

where M is the real repose angle, O is the repose angle of the model, and n is the number of simulations run per parameter. A summary of the parameters calibrated is presented in Table 3.

Table 3. Summary of calibrated parameters.

Parameter	Value	Unit
Radio inlet (circle)	0.75	m
Outlet size (rectangle)	0.12 × 0.15	m × m
Fragment sizes (min/max)	10.16/25.4	mm
Surface density	7	mm
Fragment density	2.7	t/m ³
Fragment bulk density	1.62	t/m ³
Young modulus S	1 × 10 ⁹	N/m ²
Young modulus P	1 × 10 ⁸	N/m ²
Poisson's ratio	0.3	Adim
Particle flow	80	t/h
Static friction S-P	0.53	Adim
Static friction P-P	0.62	Adim
Dynamic friction S-P	0.36	Adim
Dynamic friction P-P	0.5	Adim
Force fraction	0.4	Adim
Rolling resistance	0.3	Adim

After calibration, the numerical model was validated with the real dimension of the base case (34 m of height) simulating the discharge from the feeder. Figure 3 shows the initial segregation of coarse particles located at the external boundaries of the stockpile, while the fine particles are located mainly in the center.

In this simulation, the mean particle size difference during discharge compared between the base case and the simulation and calculated during the same discharge time was 13% (Figure 4). The error was considered acceptable based on the particle size variability and the similar tendency observed in Figure 4. In both cases (base and simulated), the particle flow begins with fine particles and then coarse particle flow follows. This phenomenon is mainly associated with initial particle segregation.

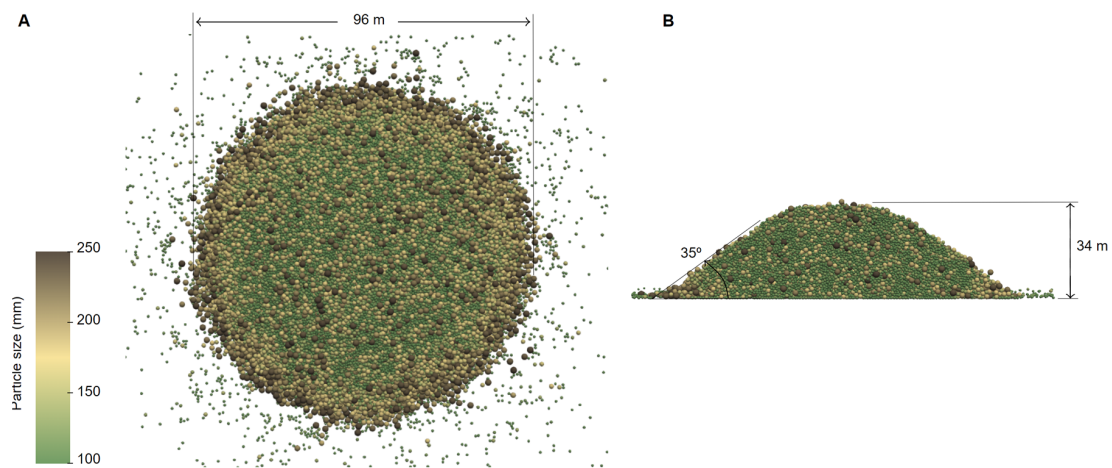


Figure 3. Large-scale stockpile in the numerical model for validation. (A) Top view. (B) Profile view in the center of the stockpile.

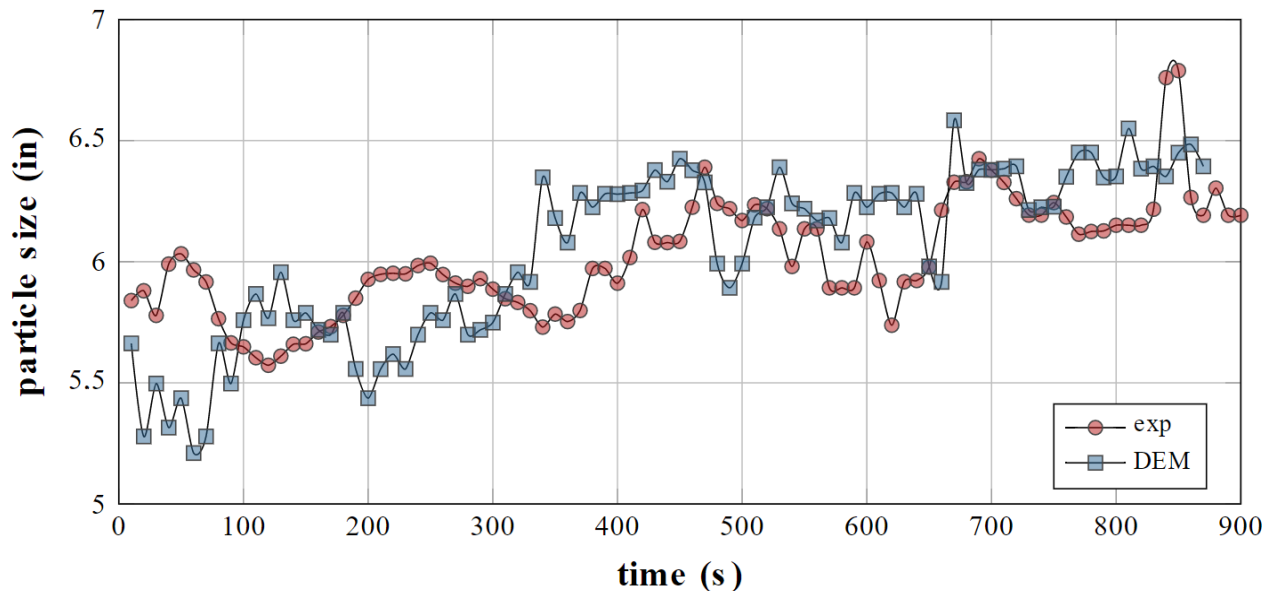


Figure 4. Mean fragment size measured during stockpiling.

4. Segregation Results and Analysis

The numerical simulation through the DEM includes stockpile loading and discharge. The live capacity is determined based on the difference between the total capacity and the mass drawn during discharge [22]. The main results are presented in Table 4. The particle shapes were modified in the last four tests. Tests 1 to 12 used sphere particles (S), test 13 used rounded cylinder particles (RC), test 14 used rounded polygon particles (RPg), test 15 used rounded polyhedrons (RPh), and test 16 used briquette particles (B).

The repose and flow angles did not necessarily increase with different particle shapes when considering the same parameter calibrated using spheres. The sphere particles were well distributed in the stockpile, resulting in a high total and live capacity. In tests 7 to 12, the effect of increasing the number of fine particles was not clear, at least within the range studied. The ore recovery from the stock increased in cases with non-spherical particle shapes.

Table 4. Numerical simulation of stockpile using the DEM.

Test	Particle Shape	Repose Angle °	Flow Angle °	Total Capacity t	Live Capacity t
1	S	31.06	44.53	0.325	23.50
2	S	30.75	42.71	0.322	23.51
3	S	30.24	41.95	0.321	23.93
4	S	31.40	45.00	0.324	23.21
5	S	30.61	44.05	0.322	23.43
6	S	30.68	40.94	0.317	23.81
7	S	31.32	44.88	0.324	23.30
8	S	30.53	43.12	0.323	23.80
9	S	30.10	42.85	0.321	23.86
10	S	31.82	43.09	0.324	22.89
11	S	30.46	43.01	0.322	23.64
12	S	28.44	40.03	0.321	24.52
13	RC	30.82	37.28	0.324	33.41
14	RPg	31.17	38.63	0.324	35.58
15	RPh	31.75	37.72	0.324	35.31
16	B	29.59	29.26	0.324	34.71

Figure 5 shows the visual particle distribution of the stockpile in tests 1 to 6, in which a coarse-to-fine particle ratio of 70/30% was modeled. The particle uniformity increased when lower feeding heights were used. Additionally, the segregation was less visible when the coefficient of uniformity was increased.

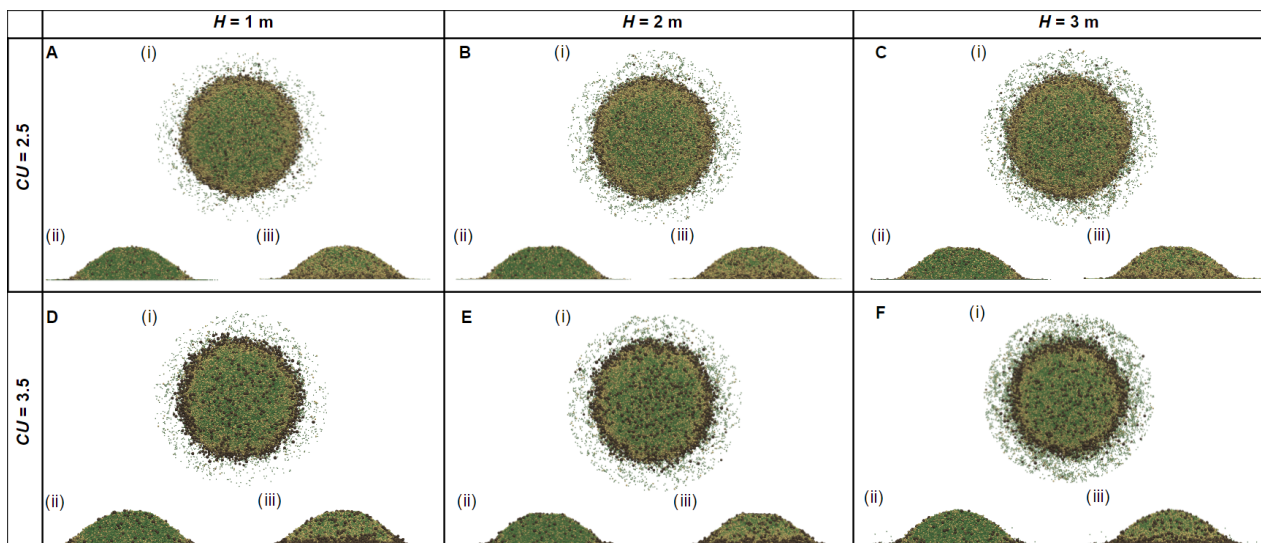


Figure 5. Different views of numerical stockpiles from tests 1 to 6. (A): Test 1, (B): Test 2, (C): Test 3, (D): Test 4, (E): Test 5, and (F): Test 6. (i) Top view, (ii) internal profile view in the center of the pile, and (iii) external profile view, respectively. Coarse particles in brown.

Figure 6 shows the visual particle distribution of the stockpile in tests 7 to 12, in which a coarse-to-fine particle ratio of 60/40% was modeled. In these tests, the number of coarse particles around the stockpile visually decreased because the percentage of coarse particles in the system was decreased. Thus, the segregation was not clearly observed compared with previous results. In the last three tests shown in Figure 6 (CU = 3.5), segregation increased slightly.

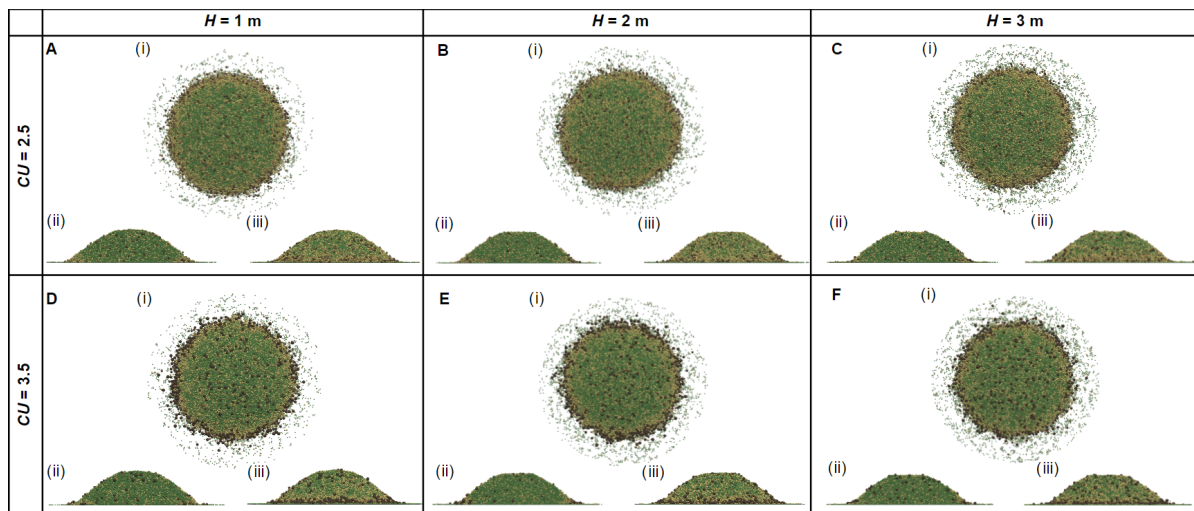


Figure 6. Different views of numerical stockpiles from tests 7 to 12. (A): Test 7, (B): Test 8, (C): Test 9, (D): Test 10, (E): Test 11, and (F): Test 12. (i) Top view, (ii) internal profile view in the center of the pile, and (iii) external profile view, respectively. Coarse particles in brown.

4.1. Segregation Coefficient

The segregation coefficient, S' , is defined in Equation (2) to compare the stockpile segregation between simulated tests. The segregation coefficient takes values between 0 and 1, where 0 represents low fine particle concentration and 1 represents high fine particle concentration in the place of measurement. This coefficient was measured in the center of the stockpile (0.4 m × 0.4 m × 0.2 m).

$$S' = \frac{n_s}{n_l v_r + n_s} \tag{2}$$

In Equation (2), n_s is the number of fine particles, n_l is the number of coarse particles, and v_r is the volumetric ratio (volume of measurement/stockpile volume). Table 5 shows the summary of the segregation coefficient measured in the 16 tests. The simulations with a segregation coefficient less than 0.9 indicate low segregation and are not representative compared with the base case. Tests 1 to 6 and 15 could effectively represent the segregation observed in the numerical model based on the consideration used in this study.

Figure 7 shows the effect of the feeding height on the segregation coefficient. The segregation coefficient decreased slightly when the feeding height was increased; however, this effect is greater when coarse-to-fine particle ratios are lower.

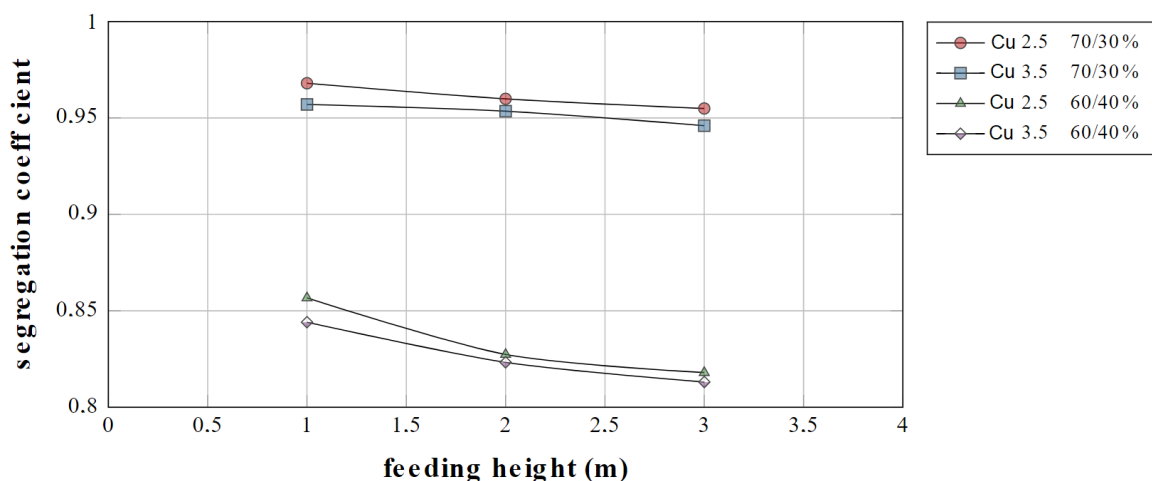


Figure 7. Height of feeding and segregation coefficient.

Table 5. Segregation coefficient measured in numerical simulation.

Test	Stockpile Volume m ³	v_r	Fine Particles in the Sample Zone	S'
1	0.158	0.203	29,872	0.968
2	0.152	0.211	28,998	0.960
3	0.149	0.215	28,498	0.955
4	0.156	0.205	27,932	0.957
5	0.151	0.212	27,680	0.953
6	0.158	0.203	26,577	0.946
7	0.155	0.206	22,389	0.857
8	0.150	0.213	20,480	0.827
9	0.148	0.217	20,009	0.818
10	0.158	0.202	20,950	0.844
11	0.150	0.213	19,989	0.823
12	0.145	0.221	19,633	0.813
13	0.152	0.210	19,946	0.865
14	0.161	0.199	19,140	0.860
15	0.158	0.203	24,966	0.926
16	0.145	0.221	12,748	0.724

4.2. Segregation during Discharge

The discharge of the stockpile from the feeder is performed by opening a space (feeder) that allows the particles to fall freely (Figure 8). The discharge ends when no more particles are falling, and the flow angle subsequently becomes defined inside the stockpile. In Figure 8, an example of the discharge is presented. Here, the fine particles are expected to start falling first, followed by the coarse particles, due to initial segregation [1,23].

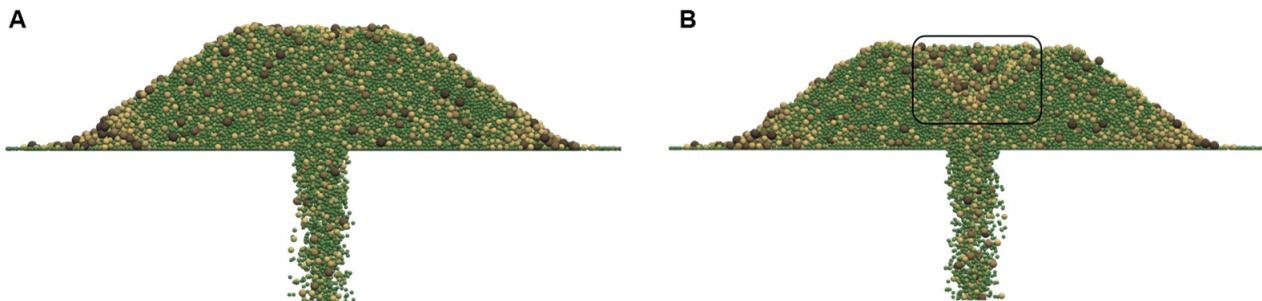


Figure 8. Example of stockpile discharge. (A) Fine particles start to flow first (green). (B) Then, the large particles (brown) begin to flow.

The mean particle size was measured during discharge in all tests, similar to the base case. Figure 9 shows the mean particle size during discharge in tests 1 to 6. These six tests show similar results that are also similar to the behavior observed in the base case (Figure 4).

Additionally, Figure 10 shows the mean particle size during discharge on tests 7 to 12, where a different ratio between coarse and fine particles was simulated. Lower mean particle size was observed, as was expected due to fewer coarse particles. Here, the discharge time was shorter at higher discharge heights. This behavior was not observed in Figure 9.

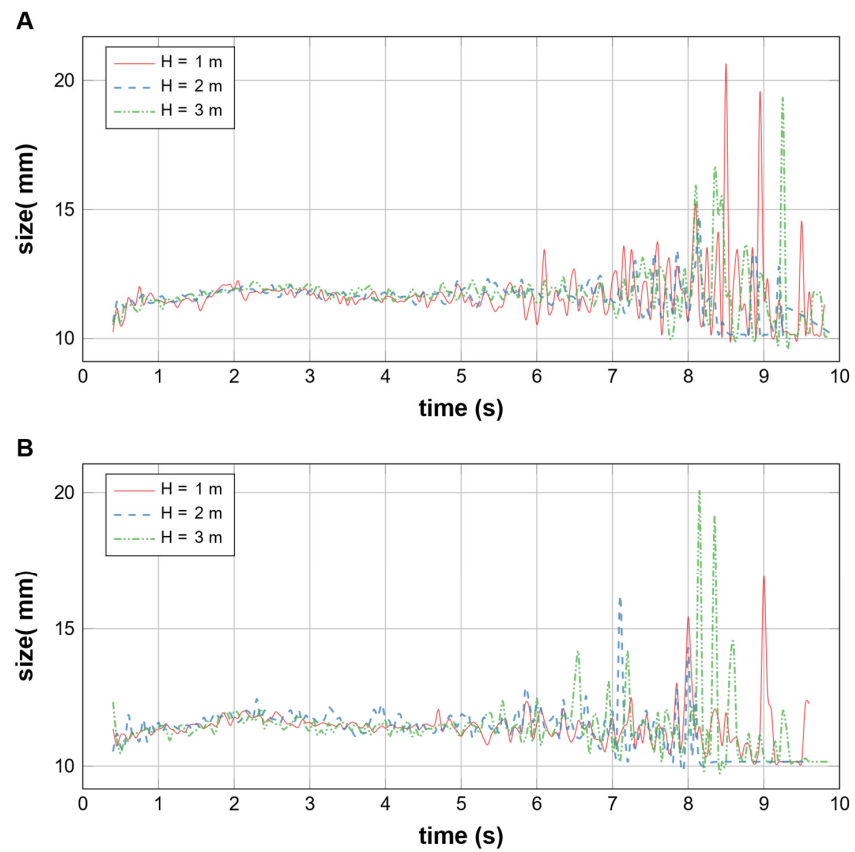


Figure 9. Mean particle size variation during discharge. (A) Tests 1–3, (B) tests 4–6.

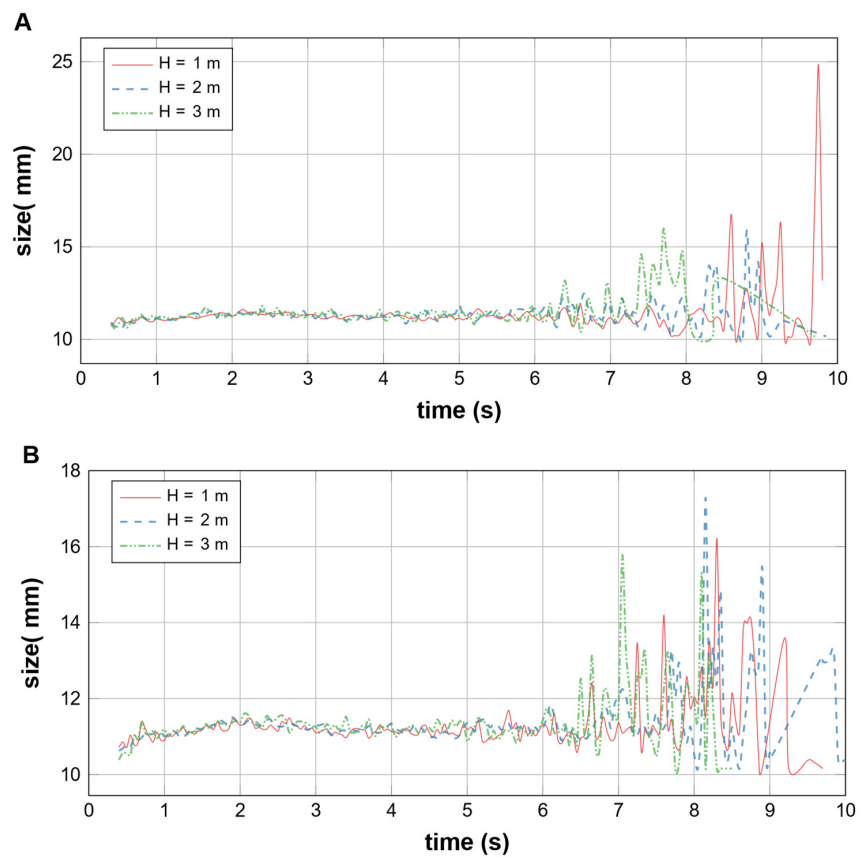


Figure 10. Mean particle size variation during discharge. (A) Tests 7–9, (B) tests 10–12.

4.3. Particle Shape Effect

In this section, the particle shape effect on stockpile segregation was analyzed. In tests 13 to 16, the shape of the particles varied compared with the setup used in test 1. Figure 11 shows the visual segregation of the stockpiles, which is less clearly observed in briquette particles (Figure 11D). The briquette particles are probably the least representative geometry of rock present in the stockpile of ore.

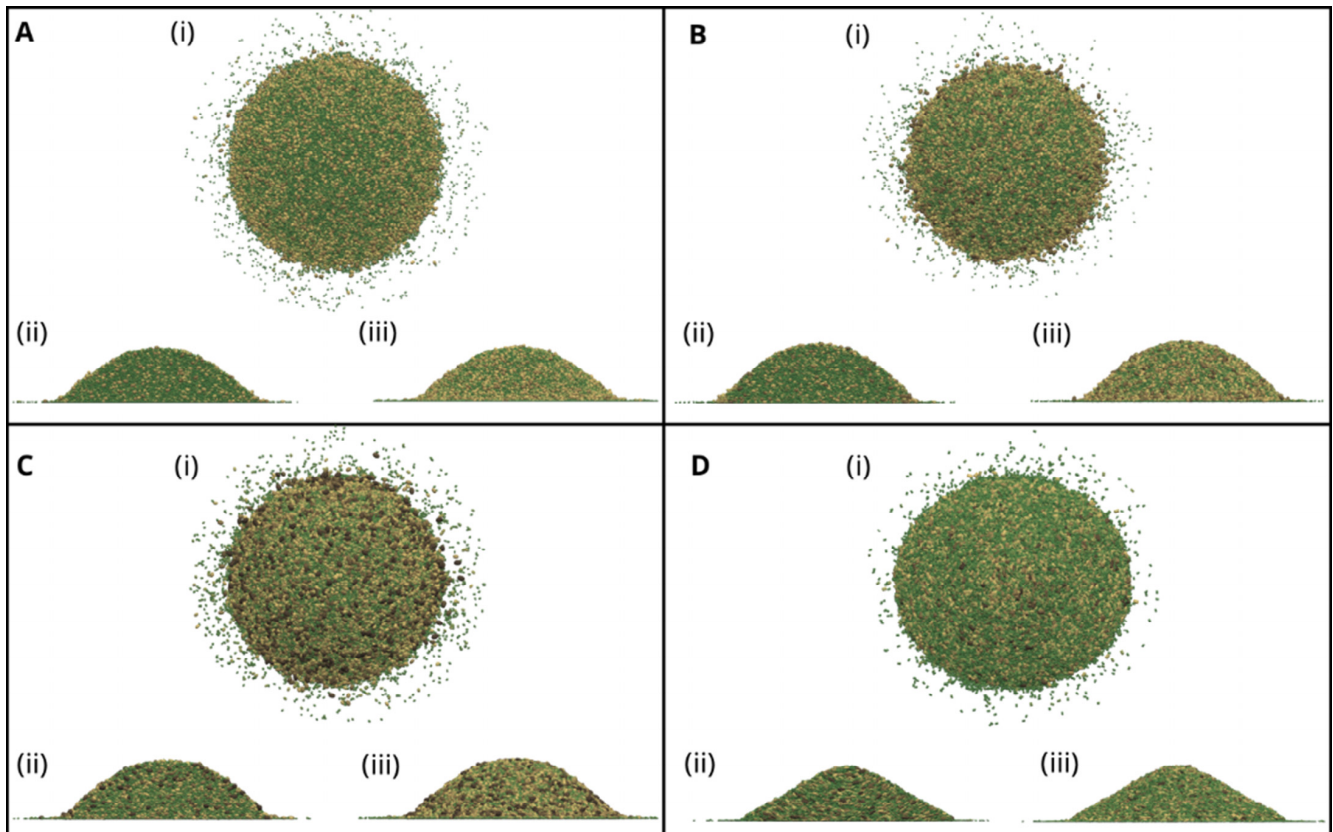


Figure 11. Numerical simulation of stockpile with different particle shapes: (A) rounded cylinder particles, (B) rounded polygon particles, (C) rounded polyhedron particles, and (D) briquette particles. (i) Top view, (ii) internal profile view in the center of the pile, and (iii) external profile view, respectively. Coarse particles in brown.

The simulation time was found to increase for some of the particle shapes tested as is summarized in Table 6. The number of faces was also directly related to the simulation time. In addition, the particle flow rate decreased with irregular geometries, such as the rounded polyhedron particles.

Table 6. Simulation time of different particle shapes.

Particle Shape	Time Simulated s	Computing Time h
S	25	~12
RC	35	~24
PgR	35	~36
PdR	35	~96
B	35	~24

5. Conclusions

In this study, it was possible to represent the natural segregation process of stockpiles of rock materials through simulations carried out using the DEM, considering the typical parameters of these materials. The particle sizes were observed to be the main parameter that influenced stockpile segregation during stockpile feeding and discharge. In terms of particle shapes, the rounded cylinder and rounded polygon shapes showed better representation of the segregation behavior during feeding, but during discharge the expected behavior was not observed. The rounded polyhedron shape showed good segregation behavior in the stockpile feeding, similar to previously calibrated spherical particles. Additionally, it was found that feeding height affects particle segregation during stockpile discharge such that particle segregation was decreased when height was increased; this is a critical factor during discharge because it directly affects the angles of repose and dumping. Then, the feeding height can be used as a design parameter to influence stockpile segregation.

Author Contributions: Conceptualization, R.C. and R.G.; methodology, M.M. and R.L.; software, M.M. and R.L.; validation, R.L.; formal analysis, R.G., K.S. and M.M.; investigation, R.G. and R.C.; resources, R.C. and K.S.; data curation, R.L.; writing—original draft preparation, R.G., M.M. and K.S.; writing—review and editing, R.G.; visualization, M.M.; supervision, R.G. and R.C.; funding acquisition, R.C. and K.S. All authors have read and agreed to the published version of the manuscript.

Funding: Raúl Castro and René Gómez were funded by Agencia Nacional de Investigación y Desarrollo, grant number AFB180004.

Institutional Review Board Statement: Not applicable.

Informed Consent Statement: Not applicable.

Data Availability Statement: Not applicable.

Acknowledgments: This paper/work was (partially) funded by the CONICYT/PIA Project AFB180004. The authors acknowledge the ESSS Group S.A. for the research license used in this project within the framework of the strategic link with the Department of Mechanical Engineering of the University of Concepción. The authors thank Diane Greenstein for her support in editing.

Conflicts of Interest: The authors declare no conflict of interest.

Nomenclature

B	Briquette particles
CU	Coefficient of uniformity (d_{60}/d_{10})
DEM	Discrete element method
H	Feeding height
M	Real repose angle
n_s	number of fine particles
n_l	number of coarse particles
n	number of simulations
O	Observed repose angle
PSD	Particle size distribution
RC	Rounded cylinder particles
RPg	Rounded polygon particles
RPh	Rounded polyhedron particles
S	Sphere particle
S'	Segregation coefficient
v_r	volumetric ratio (volume of measurement/stockpile volume)

References

1. Zhang, D.; Zhou, Z.; Pinson, D. DEM simulation of particle stratification and segregation in stockpile formation. *EPJ Web Conf.* **2017**, *140*, 15018. [[CrossRef](#)]
2. Yahyaeei, M.; Ye, Z.; Hilden, M.; Ruitz, E.A.; Gavelan, Z. Investigating the size segregation of stockpile at MMG's Las Bambas and its impact on performance of SAG mills. In Proceedings of the Mill Operators 2021, Brisbane, Australia, 23–25 June 2021; Australian Institute of Mining and Metallurgy: Brisbane, Australia, 2021.
3. Cabrejos, F. Effect of moisture content on the flowability of crushed ores. *EPJ Web Conf.* **2017**, *140*, 8011. [[CrossRef](#)]
4. Ye, Z.; Yahyaeei, M.; Hilden, M.M.; Powell, M.S. A laboratory-scale characterisation test for quantifying the size segregation of stockpiles. *Miner. Eng.* **2022**, *188*, 107830. [[CrossRef](#)]
5. Lu, T.F.; Xu, S. SPSim: A stockpile simulator for analyzing material quality distribution in mining. In Proceedings of the 2010 IEEE International Conference on Mechatronics and Automation, ICMA 2010, Xi'an, China, 4–7 August 2010; pp. 299–304.
6. de Castro, M.H.; da Luz, J.A.M.; de Orquiza Milhomem, F. Cellular automaton-based simulation of bulk stacking and recovery. *J. Mater. Res. Technol.* **2022**, *16*, 263–275. [[CrossRef](#)]
7. Ye, Z.; Hilden, M.M.; Yahyaeei, M. A 3D cellular automata ore stockpile model—Part 1: Simulation of size segregation. *Miner. Eng.* **2022**, *187*, 107816. [[CrossRef](#)]
8. Michot-Roberto, S.; Garcia-Hernández, A.; Dopazo-Hilario, S.; Dawson, A. The spherical primitive and perlin noise method to recreate realistic aggregate shapes. *Granul. Matter* **2021**, *23*, 41. [[CrossRef](#)]
9. Mollon, G.; Quacquarelli, A.; Andò, E.; Viggiani, G. Can friction replace roughness in the numerical simulation of granular materials? *Granul. Matter* **2020**, *22*, 42. [[CrossRef](#)]
10. Yu, Y.; Zhang, J.; Zhang, J.; Saxén, H. DEM and experimental studies on pellet segregation in stockpile build-up. *Ironmak. Steelmak.* **2018**, *45*, 264–271. [[CrossRef](#)]
11. Vuilloz, T.; Cantor, D.; Ovalle, C. DEM modeling of segregation and stratification in pouring heaps of bidispersed mixtures of rounded particles. *EPJ Web Conf.* **2021**, *249*, 03049. [[CrossRef](#)]
12. Adjiski, V.; Panov, Z.; Popovski, R.; Stefanovska, R.K. Discrete Element Method (DEM) for segregation analysis of granular materials: Analysis of stockpile formed by conveyor belt. *Nat. Resour. Technol.* **2020**, *14*, 19–26. [[CrossRef](#)]
13. Cundall, P.A.; Strack, O.D.L. A discrete numerical model for granular assemblies. *Geotechnique* **1979**, *29*, 47–65. [[CrossRef](#)]
14. ESSS Rocky DEM 2022. Available online: <https://rocky.esss.co/software/> (accessed on 28 November 2022).
15. Moncada, M.; Toledo, P.; Betancourt, F.; Rodríguez, C. Torque Analysis of a Gyratory Crusher with the Discrete Element Method. *Minerals* **2021**, *11*, 878. [[CrossRef](#)]
16. Chitalov, L.S.; Lvov, V.V. New approaches in mineral raw materials comminution tests modelling. In *Advances in Raw Material Industries for Sustainable Development Goals*; Litvinenko, V., Ed.; CRC Press: Boca Raton, FL, USA, 2020; p. 6. ISBN 9781003164395.
17. Venegas, J.; Valenzuela, M.A.; Molina, C. Correlation Between Power and Lifters Forces in Grinding Mills. *IEEE Trans. Ind. Appl.* **2018**, *55*, 4417–4427. [[CrossRef](#)]
18. Ilic, D.; Roberts, A.; Wheeler, C.; Katterfeld, A. Modelling bulk solid flow interactions in transfer chutes: Shearing flow. *Powder Technol.* **2019**, *354*, 30–44. [[CrossRef](#)]
19. Pereira, G.; Magalhães, R.; Pastro, B. Applying Discrete Element Method to the simulation of iron ore pellets loading in double-hatch hold ships. In Proceedings of the 37th Logistics Seminar—Supplies, PCP, Transport, Sao Paulo, Brazil, 2–4 October 2018.
20. Kasmaee, S.; Tinti, F.; Bruno, R. Characterization of metal grades in a stockpile of an Iron Mine (Case study-Choghart iron mine, Iran). *Rud. Zb.* **2018**, *33*, 51–60. [[CrossRef](#)]
21. Samadani, A.; Pradhan, A.; Kudrolli, A. Size segregation of granular matter in silo discharges. *Phys. Rev. E* **1999**, *60*, 7203. [[CrossRef](#)] [[PubMed](#)]
22. Ferreira, T.R.; da Luz, J.A.M.; de Castro, M.H. Live volume of conical stockpile reclaimed by gravity. *Res. Soc. Dev.* **2022**, *11*, e13511628908. [[CrossRef](#)]
23. Cabrejos-Marín, F. Gravity reclaim stockpiles: What you need to know. *Part. Sci. Technol.* **2018**, *36*, 473–480. [[CrossRef](#)]